Published in final edited form as:

Vet Comp Oncol. 2011 September ; 9(3): 207–218. doi:10.1111/j.1476-5829.2010.00249.x.

Protein kinase C regulates ezrin–radixin–moesin phosphorylation in canine osteosarcoma cells

S.-H. Hong[1], **T. Osborne**[1], **L. Ren**[1], **J. Briggs**[1], **C. Mazcko**[2], **S. S. Burkett**[3], **C. Khanna**[1,2]

[1]Tumor and Metastasis Biology Section, Pediatric Oncology Branch, Center for Cancer Research, National Cancer Institute, National Institutes of Health, Bethesda, MD, USA

[2]Comparative Oncology Program, Center for Cancer Research, National Cancer Institute, National Institutes of Health, Bethesda, MD, USA

[3]Comparative Molecular Cytogenetics Core, Mouse Cancer Genetics Program, National Cancer Institute, National Institutes of Health, Frederick, MD, USA

Abstract

The development of metastasis is the most significant cause of death for both canine and human patients with osteosarcoma (OS). Ezrin has been associated with tumour progression and metastasis in human, canine and murine OS. Ezrin activation is dynamically regulated by protein kinase C (PKC) during metastatic progression in human and murine OS. To include the dog in the development of therapeutics that target ezrin biology, we characterized four new canine OS cell lines and confirmed the relationship between PKC and ezrin in these cells. Three of four cell lines formed tumours in mice that were histologically consistent with OS. All cell lines were markedly aneuploid and expressed ezrin and PKC. Finally, both ezrin phosphorylation and cell migration were inhibited using a PKC inhibitor. These data suggest that an association between PKC-mediated activation of ezrin and the metastatic phenotype in canine OS cells.

Keywords

dog; ezrin; metastasis; osteosarcoma; PKC

Introduction

Osteosarcoma (OS) is the most common malignant primary bone tumour in dogs as well as humans.[1–4] Spontaneously occurring canine OS, unlike induced tumours of rodent model systems, closely resembles human OS in its histological appearance, biological behaviour and response to therapy.[2,4–6] Recent gene expression studies further suggest strong similarities between dog and human OS.[7,8] Despite effective management of the primary tumour, the development of metastasis continues to be the most significant cause of death in both species.

Correspondence address: S.-H. Hong, Tumor and Metastasis, Biology Section, Pediatric Oncology Branch, Center for Cancer Research, National Cancer Institute, National Institutes of Health, 37 Convent Drive, Bethesda, MD 20892, USA, hongsu@mail.nih.gov.

We have previously reported that ezrin, a membrane-actin cytoskeleton linker protein, is necessary for the metastatic phenotype by providing an early survival advantage for OS cells that reach the lung.[9] Ezrin plays a key role in the coordination of signals and cellular complexes that are required for the successful metastasis of many tumour types.[10,11] Ezrin is a member of the ezrin–radixin–moesin (ERM) protein family, within the protein 4.1 superfamily.[12] Ezrin is involved in the determination of cell shape, cell adhesion, motility and signal transduction. Phosphorylation of a critical threonine residue (T567) in the c-terminus of ezrin results in a conformational opening of its protein structure that then allows the c-terminus of ezrin to bind the actin cytoskeleton and the n-terminus of ezrin to bind to the cell membrane or membrane-associated proteins. It is believed that this linkage allows for a physical connection between the cell membrane and the actin cytoskeleton that is necessary for metastasis. The linkage also promotes coordination of signalling events from membrane-associated receptors, resulting in increased efficiency and/or amplification of signal transduction.[12] Indeed, mutation of T567, in both OS and rhabdomyosarcoma, abrogates the ezrin-dependent effects on metastasis.[13,14] We have found ezrin expression in most human cancers, with aberrant expression most notably evident in cancers of mesenchymal origin.[15] The linkage between ezrin expression and cancer progression and metastasis has been demonstrated in a variety of cancers including rhabdomyosarcoma, Ewings sarcoma, soft tissue sarcoma, melanoma and brain tumours.[14,16 – 19] Recently, we reported that ezrin is not maintained in an active phosphorylated form throughout metastatic progression.[13] Phosphorylation of ezrin is seen in cancer cells early after their arrival in the lung and late as metastatic lesions progress into the surrounding microenvironment. In addition, ezrin phosphorylation is dynamically regulated during murine and human OS metastasis by PKC. We hypothesize that targeting PKC activation of ezrin during specific times in metastatic progression may be considered a means to improve outcome for patients with metastasis.[13] Such translational development of a therapeutic approach targeting metastatic progression in OS, would be optimized by the inclusion of dogs with naturally occurring OS.

In this study, we report on the characterization of four novel cell lines from dogs with OS. We found ezrin expression in all four canine OS cells lines. Furthermore, as in other species, the phosphorylation of ezrin was regulated by PKC. Finally, pharmacological inhibition of PKC resulted in decreased motility of these cell lines. These data support an association between PKC-mediated activation of ezrin in the metastatic phenotype of canine OS cells and suggest the continued opportunity to include canine OS in the development of novel therapeutic approaches targeting the activation of ezrin in OS metastasis.

Materials and methods

Establishment of canine OS cell lines

The canine OS cell lines were derived at the time of definitive resection (amputation) of the primary tumour (Table 1). Primary tumour tissues were obtained from the amputated limb under aseptic conditions. The tissues were washed three times with Dulbecco’s modified Eagle’s medium (DMEM) (Invitrogen, Carlsbad, CA, USA) culture media containing 10% foetal bovine serum, penicillin (100 units/mL) and streptomycin (100 μg/mL, Invitrogen,

Carlsbad, CA, USA) and minced into small fragments. Tumour tissues were placed into filtered screw-top culture flasks (Nunc, Rochester, NY, USA) moistened with medium. The flasks were cultured at 37 °C in a 5% CO_2 incubator for 2 h, allowing cell adherence. Then a small amount of DMEM containing 10% foetal bovine serum, L-glutamine (2 mmol), penicillin (100 units/mL) and streptomycin (100 μg/mL, Invitrogen, Carlsbad, CA, USA) was added. The culture medium was changed every other day until flasks were confluent. The cells were split into new culture flasks using 0.05% trypsin–EDTA (Invitrogen, Carlsbad, CA, USA).

Canine OS cell line characterization

In vitro cell proliferation assay

Cell growth was analysed using a CCK-8 assay according to manufacturers instructions (Dojindo Molecular Technologies, Rockville, MD, USA). Briefly, cells were plated in pentuplicate in 96-well plates (2500 cells/well). At the indicated time points, the CCK-8 reagent was added to the medium at a ratio with 1:10. The cells were incubated for 2 h at 37 °C in incubator. Optical density values were measured at 450 nm in a microplate reader (Molecular Devices, Sunnyvale, CA, USA).

Karyotype analysis

Karyotype analysis was completed as previously described.[20] Briefly, cultured cells were arrested in the metaphase stage of cellular division by incubating with Colcemid (KaryoMax® Colcemid Solution, Invitrogen, Carlsbad, CA, USA) (10 μg/mL) for 2 h prior to harvest. Cells were dissociated with 0.05% trypsin/EDTA (Invitrogen, Carlsbad, CA, USA), treated with hypotonic solution (KCL 0.075 M) for 15 min at 37 °C and fixed with methanol: acetic acid 3:1. Five metaphase cells were analysed for each cell line. Chromosomes were stained with a trypsin-Giemsa staining technique and karyotyped using an Axioplan 2 microscope (Carl Zeiss MicroImaging, Thornwood, NY, USA) coupled with a charge-coupled device camera (Photometrics, Tucson, AZ, USA), and images were captured with Band View 5.5 karyotyping software (Applied Spectral Imaging, Vista, CA, USA).

In vivo primary tumour growth, experimental and spontaneous metastasis assay

For assessment of primary tumour growth and spontaneous metastasis, two million canine tumour cells were injected to a paraoseous location, adjacent to the left proximal tibia in 4-week-old female severe combined immune-deficient (SCID)/Beige mice (Charles River Laboratories International, Wilmington, MA, USA).[21] For assessment of experimental metastasis, one million cells were introduced by tail vein injection in 4-week-old female SCID/Beige mice.[21] Primary tumour endpoints included: time to detection of tumour, percent tumour take and tumour growth. When primary tumours reached 1.5 cm, the tumour-bearing limb was surgically resected. Mice were then monitored for evidence of spontaneous metastasis and morbidity associated with pulmonary metastasis. Mice were euthanized based on the development of these symptoms. Necropsies were performed on all mice to confirm the presence of metastatic lung disease. Endpoints for experimental metastasis assays were similar. Animal care and use were in accordance with the guidelines of the NIH Animal Care and Use Committee.

Histopathology and immunohistochemistry

Primary tumour tissues were obtained at the time of amputation and the entire lung was harvested from mice at the time of euthanization. Primary tumour tissues were fixed in 10% formalin in neutral buffer overnight, no longer than 24 h, and then transferred to 80% ethanol. Lungs were insufflated by tracheobronchial injection of 1 mL neutral buffered 10% formalin fixed for 24 h, and then transferred to 80% ethanol. The tissues were embedded in paraffin, sectioned at 5 μm thickness and mounted on the glass slides. Slides were deparaffinized and rehydrated as previously described.[22] The tumour tissue sections were stained with haematoxylin and eosin (H&E) and examined with a light microscope. Immunohistochemistry for Alkaline Phosphatase (ALP) was undertaken as previously described.[13] Briefly, slides were incubated in preheated target retrieval solution (Dako, Carpinteria, CA, USA), pH 6, in a steam cooker for 20 min. Anti-ALP antibody (Abcam, Cambridge, MA, USA) was used at 1:50 dilution. The samples were counter-stained with haematoxylin (Dako, Carpinteria, CA, USA) for 30 s, mounted and examined by light microscopy.

Western blot analysis

Cells were lysed in either sodium dodecyl sulfate (SDS) or radio-immuno precipitation assay buffer (150 mM NaCl, 50 mM Tris, pH 8.0, 0.1% SDS, 0.5% deoxycholate, 1% NP-40) with proteinase inhibitor cocktail (Roche Diagnostics, Indianapolis, IN, USA). Protein lysates (20–40 μg/lane), as determined by DC protein assay (Bio-Rad Life Science, Hercules, CA, USA), were separated by SDS-PAGE using 4–20% Tris–glycine gels and transferred to a nitrocellulose membrane (Invitrogen, Carlsbad, CA, USA). The membranes were blocked with 5% nonfat dried milk in TBS-Tween-20 (20 mmol/L Tris–HCl, pH 7.5, 8 g/L of sodium chloride, 0.1% Tween-20) and then incubated with anti-ezrin (1:4000 dilution) (Sigma, St Louis, MO, USA), anti-ERM (1:1000 dilution) (Cell Signaling, Beverly, MA, USA), anti-phosphorylated ERM (1:1000 dilution) (Cell Signaling, Beverly, MA, USA), anti-PKCα (1:1000 dilution) (Upstate, Swampscott, MA, USA), anti-PKCγ (1:1000 dilution) (BD Biosciences, Palo Alto, CA, USA), anti-PKCι (1:250 dilution) (BD Biosciences, Palo Alto, CA, USA), anti-phosphorylated Akt (1:1000 dilution) (Cell Signaling, Beverly, MA, USA), anti-Akt (1:1000 dilution) (Cell Signaling, Beverly, MA, USA) or anit-β-actin (1:10 000 dilution) (Sigma, St Louis, MO, USA) overnight at 4 °C. After incubation, the membranes were washed and antibody binding was visualized by exposure to a 1:20 000 dilution of an anti-rabbit IgG HRP-linked antibody (Pierce, Rockford, IL, USA) or anti-mouse IgG HRP-linked antibody (Pierce, Rockford, IL, USA) for 1 h at 37 °C and developed by SuperSignal West Pico Chemiluminescent Substrate (Pierce, Rockford, IL, USA) detection and subsequent exposure to film.

Kinase inhibitor treatments

An equal number of cells were plated in six-well tissue culture plates, grown to 70% confluence and then treated with the pharmacological inhibitor for PKC, Ro31–8220 (Alexis Biochemicals, Lausen, Switzerland). Dose titration (0, 0.1, 1, 5, 10 μM) at 1 h and time course study (0, 10, 30, 60, 120 min) at 5 μM were performed. Dimethylsulphoxide was used as the control for the treatments. The treated cells were lysed in 200 μl of 1X

Laemmli's buffer. Western blot analysis was performed on cell lysates from these treated cells using anti-phosphorylated ERM (1:1000 dilution) and anti-phosphorylated Akt (Ser473) antibodies.

Wound-healing cell migration assay

Each canine OS cell line was plated in six-well tissue culture dishes (Nunc, Rochester, NY, USA) at near confluence in complete medium. A 'wound' was made by scraping with a P200 pipette tip in the middle of the cell monolayer. Floating cells were removed by washing with phosphate-buffered saline and fresh complete medium containing dimethylsulphoxide, 0.1 or 1 μM Ro31–8220 (Alexis Biochemicals, Lausen, Switzerland) was added. Cells were incubated at 37 °C for 13 h (KOS-001, KOS-003 and KOS-004) or 24 h (KOS-002). Phase contrast images were then taken using a Leica DMIRB inverted microscope.

Results

Morphology and *in vitro* cell proliferation

KOS-001 cells were variably sized spindloid to elongate cells that contained small amounts of cytoplasm and had angular borders (Fig. 1A). These cells contained a single large, eccentric, round to oval nucleus with finely stippled chromatin and one to two prominent nucleoli. In addition, many cells had long cytoplasmic extensions. KOS-002 cells were variably sized mostly angular to stellate cells interspersed with some spindloid cells (Fig. 1B). A single large, round, centrally located nucleus was present with finely stippled chromatin and a single central nucleolus. These cells often had multiple short cytoplasmic extensions. KOS-003 and KOS-004 cells were variably sized spindloid to elongate cells with fewer angular cells (Fig. 1C,D). These cells had either a single long cytoplasmic extension or multiple short cytoplasmic extensions. Nuclei were large, round to oval, eccentrically located, with finely stippled chromatin. Occasionally centrally located nucleoli were present. Rarely KOS-003 cells had multiple nuclei. Using CCK8 enumeration of cells, growth curves for all canine OS cells were developed (Fig. 1E) and doubling times determined. The doubling times of KOS-001, KOS-002, KOS-003 and KOS-004 were 19.8, 24.7, 16.0 and 12.1 h respectively.

Karyotype analysis

The karyotype of all canine OS cell lines was analysed by Giemsa trypsin banding. The karyotype of each canine OS cell line was complex and bizarre with multiple translocations and other cytogenetic abnormalities (Fig. 1F). The number of chromosomes of KOS-001 cells ranged from 97 to 105 (mode number was 101). KOS-002, KOS-003 and KOS-004 were also abnormal with chromosome range from 87 to 95 (mode number was 95), from 81 to 82 (mode number was 81) and from 96 to 103 (mode number was 103), respectively.

In vivo primary tumour growth, experimental and spontaneous metastasis

KOS-001, KOS-003 and KOS-004 cells developed primary tumours after paraoseous injection in immuno compromised mice(Fig. 2). Mice receiving KOS-002 did not develop primary tumours followed 1 year after injection (Table 2). On histological examination hind

limbs contained unencapsulated, but well-demarcated masses that invaded and replaced the musculature and adjacent bone in all three canine OS cells (Fig. 2B,E,H). Neoplastic cells were arranged in closely packed streams and bundles supported by a fibrous stroma. Individual cells were mainly elongated spindle cells with some round to polygonal cells scattered throughout. Cell borders were often indistinct and contained scant to moderate amounts of eosinophilic to amphophilic cytoplasm. Nuclei were eccentric, round to oval with a hypochromatic to euchromatic chromatin staining pattern and finely stippled to coarsely clumped chromatin distribution. One to three prominent, round, basophilic nucleoli were present in most cells. Small to moderate amounts of faintly to intensely eosinophilic, hyaline material (osteoid) was arranged in narrow ribbons to small irregular islands between malignant cells. Strong ALP expression was detected in primary tumours (KOS-001, KOS-004 and KOS-003, Fig. 2C,F,I).

Following resection of the primary tumour-bearing limb in mice receiving KOS-003 cells, pulmonary metastasis developed within 30 days (Table 2 and Fig. 3A). None of the mice receiving KOS-001 and KOS-004 developed metastasis following tumour-bearing limb resection through a 1-year period of observation (Table 2 and Fig. 3A).

Consistent with results for spontaneous metastasis, experimental metastases were present only in the KOS-003 cells. The median survival (death because of morbidity of pulmonary metastasis) for these mice was 49 days (Fig. 3B). Pulmonary metastases from both experimental and spontaneous metastasis were diffuse and widespread. Lung metastases had a similar histo-morphological appearance to the primary tumours, including islands of osteoid and strong ALP expression (KOS-003, Fig. 3C,F).

Ezrin and PKC isoforms α, γ and ι are expressed in canine OS

To determine the protein expression of ezrin and PKC isoforms α, γ and ι in canine OS cells, Western blot analysis was performed including K7M2 murine OS cells lysates as a positive control.[13] As shown in Fig. 4A,B, ezrin and PKC isoforms α, γ and ι were expressed in all canine OS cell lines.

PKC regulates ezrin Thr567 phosphorylation (activation) in canine OS cells

To test the hypothesis that PKC phosphorylates ezrin at threonine 567 in canine OS cells, a pharmacological inhibitor of PKC, Ro31–8220, was used. As shown in Fig. 5, Ro31–8220 suppressed c-terminal phosphorylation of ERM proteins in a dose- and time-dependent manner. In contrast, Akt (Ser473) phosphorylation was not affected by PKC inhibitor treatment even at the highest dose–time exposures of 5 μM over 120 min.

PKC-mediated tumour cell migration in wound-healing cell migration assay

To verify the biological significance of PKC regulation on ERM phosphorylation, we examined the effects of PKC inhibition on cell motility using a standard wound-healing assay for cell migration. Cellular motility was assessed over 13 h (KOS-001, KOS-003 and KOS-004) or 24 h (KOS-002). Dose and time-point combinations were selected to minimize any potential effects of PKC inhibition on cell proliferation and viability. Images of the ‘wound’ were taken immediately (time 0) and 13 or 24 h post-wounding. As shown in Fig.

6, the cells treated with the PKC inhibitor, Ro31–8220, had a significant delay in migration compared with control groups.

Discussion

We have established and characterized four canine OS cell lines using both vitro and *in vivo* assessments of tumour biology. The morphological phenotype of these cells was mesenchymal. The karyotypic features supported their canine origin, and the complex and markedly aneuploid chromosomal number and arrangement were characteristic of OS.[23] Histological features of xenograft tumours were consistent with OS with the presence of atypical sarcoma cells producing tumour osteoid and expressing ALP. Following orthotopic growth in mice, one of the established canine OS cell lines formed spontaneous pulmonary metastasis within 1 month of resection of the tumour-bearing limb. This panel of cell lines will provide important opportunities to study the complexity of OS biology and therapy. Indeed, in this report we specifically applied these cell lines to study the connection between the metastasis-associated protein, ezrin and PKC. All four OS cell lines expressed ezrin and classical PKC family members. The phosphorylation of ezrin and cellular motility was inhibited using a specific and previously described inhibitor of PKC in these canine cells. These data support the continued inclusion of canine OS in the development of novel therapeutics that target the ezrin–PKC phenotype in metastatic progression.

We have previously published that ezrin phosphorylation is dynamically regulated during metastasis in murine and human OS.[13] Ezrin is expressed in a phosphorylated form early after metastatic cells arrive in the lung. This active conformation of ezrin is believed to be necessary for OS cells to overcome the inefficiency of metastasis that occurs early after metastatic cells arrive at a secondary site. We hypothesize that ezrin protects cells from the stresses experienced by cells as they arrive in this foreign microenvironment. After successful metastatic lesion progress from the single cell to multiple cell level, we were surprised to find that ezrin, although consistently expressed, was no longer phosphorylated. As the metastatic lesions progressed and cells began to engage the lung parenchyma, ezrin again became phosphorylated most notably at the periphery of the metastatic lesion. Through a number of techniques we have demonstrated that this dynamic regulation of ezrin phosphorylation is the result of classical PKC family members.[13] Finally, some of the recognized effects of PKC on cell motility and invasion were shown to be dependent on ezrin activation.[24–26] These data suggested an opportunity to develop therapeutic strategies for cancer metastasis that target the ezrin–PKC phenotype.

An important hurdle that exists in the development of PKC-based therapeutics for cancer has been toxicity.[27] This problem has been managed through increasingly selective inhibitors of PKC and the development of treatment schedules that are tolerable in patients. Small molecule inhibitors of PKC have now successfully moved into phase II clinical trials in human patients for a number of indications.[28,29] On the basis of our interest in PKC, ezrin and metastasis, it is reasonable that some of the toxicity concerns linked to long-term high-dose exposures to PKC inhibitors may be managed through intermittent dosing that may effectively interrupt the dynamic regulation of PKC on ezrin seen during metastasis. An optimal drug development path based for PKC inhibitors used in this manner requires the

development of informative pharmacodynamic biomakers, and a means to model the complexity of metastatic progression from a period of minimal residual disease to gross metastasis. The inclusion of pet dogs with OS into such a development path would provide an opportunity to model this biology and answer questions that are difficult to answer in conventional preclinical models or in human patients. The outcome of such a successful development path could be more effective treatments for both canine and human patients with OS.

To extend our understanding of PKC-mediated ezrin phosphorylation to canine OS, we report herein on the expression of ezrin and PKC family members in canine OS cells and the regulation of ezrin phorphorylation by PKC. All four canine OS cell lines expressed ezrin, other ERM proteins and PKC α, γ and ι. The levels of expression were comparable to a previously characterized and metastatic murine model of OS (K7M2). It is interesting to note that the, highly aggressive KOS-003 showed lower expression of some PKC isoforms, compared with other cells. It is unclear what threshold of PKC isoforms expression is necessary to convey a 'PKC functional status' to a cell. These data further support the recognized concept that the expression of a single protein is not sufficient to account for the phenotype of a metastatic cancer cell. Using a small molecule PKC inhibitor, we found down regulation of phosphorylated ERM in dose- and time-dependent manner. The specificity of this effect was confirmed by lack of effect on the phosphorylation status of the Akt pathway. In addition, using wound-healing migration assay as an example of a PKC-related metastatic phenotype, we found significant inhibition of cellular migration following identical exposure to the small molecule inhibitor of PKC.

In conclusion, using four newly established canine OS cell lines we have demonstrated that the connection between PKC and ezrin is linked to the biology of canine OS. Specifically, PKC is responsible for the phosphorylation of ezrin and cell migration in canine OS cells. These data support the continued study of novel therapeutic approaches that target the ezrin–PKC phenotype in canine OS.

Acknowledgements

This project was supported by a grant (1046-A) from the American Kennel Club Canine Health Foundation. The contents of this publication are solely the responsibility of the authors and do not necessarily represent the views of the Foundation.

References

1. Bruland OS and Pihl A. On the current management of osteosarcoma. A critical evaluation and a proposal for a modified treatment strategy. European Journal of Cancer 1997; 33: 1725–1731. [PubMed: 9470825]
2. MacEwen EG. Spontaneous tumors in dogs and cats: models for the study of cancer biology and treatment. Cancer and Metastasis Reviews 1990; 9: 125–136. [PubMed: 2253312]
3. Meyers PA and Gorlick R. Osteosarcoma. Pediatric Clinics of North America 1997; 44: 973–989. [PubMed: 9286295]
4. Withrow SJ, Powers BE, Straw RC and Wilkins RM. Comparative aspects of osteosarcoma. Dog versus man. Clinical Orthopaedics and Related Research 1991; 270: 159–168.
5. Mueller F, Fuchs B and Kaser-Hotz B. Comparative biology of human and canine osteosarcoma. Anticancer Research 2007; 27: 155–164. [PubMed: 17352227]

6. Khanna C, Lindblad-Toh K, Vail D, London C, Bergman P, Barber L, Breen M, Kitchell B, McNeil E, Modiano JF, Niemi S, Comstock KE, Ostrander E, Westmoreland S and Withrow S. The dog as a cancer model. Nature Biotechnology 2006; 24: 1065–1066.
7. Paoloni M, Davis S, Lana S, Withrow S, Sangiorgi L, Picci P, Hewitt S, Triche T, Meltzer P and Khanna C. Canine tumor cross-species genomics uncovers targets linked to osteosarcoma progression. BMC Genomics 2009; 10: 625. [PubMed: 20028558]
8. Selvarajah GT, Kirpensteijn J, van Wolferen ME, Rao NA, Fieten H and Mol JA. Gene expression profiling of canine osteosarcoma reveals genes associated with short and long survival times. Molecular Cancer 2009; 8: 72. [PubMed: 19735553]
9. Khanna C, Wan X, Bose S, Cassaday R, Olomu O, Mendoza A, Yeung C, Gorlick R, Hewitt SM and Helman LJ. The membrane-cytoskeleton linker ezrin is necessary for osteosarcoma metastasis. Nature Medicine 2004; 10: 182–186.
10. Elliott BE, Meens JA, SenGupta SK, Louvard D and Arpin M. The membrane cytoskeletal crosslinker ezrin is required for metastasis of breast carcinoma cells. Breast Cancer Research 2005; 7: R365–R373. [PubMed: 15987432]
11. Hunter KW. Ezrin, a key component in tumor metastasis. Trends in Molecular Medicine 2004; 10: 201–204. [PubMed: 15121044]
12. Bretscher A, Edwards K and Fehon RG. ERM proteins and merlin: integrators at the cell cortex. Nature Reviews. Molecular Cell Biology 2002; 3: 586–599. [PubMed: 12154370]
13. Ren L, Hong SH, Cassavaugh J, Osborne T, Chou AJ, Kim SY, Gorlick R, Hewitt SM and Khanna C. The actin-cytoskeleton linker protein ezrin is regulated during osteosarcoma metastasis by PKC. Oncogene 2009; 28: 792–802. [PubMed: 19060919]
14. Yu Y, Khan J, Khanna C, Helman L, Meltzer PS and Merlino G. Expression profiling identifies the cytoskeletal organizer ezrin and the developmental homeoprotein six-1 as key metastatic regulators. Nature Medicine 2004; 10: 175–181.
15. Bruce B, Khanna G, Ren L, Landberg G, Jirstrom K, Powell C, Borczuk A, Keller ET, Wojno KJ, Meltzer P, Baird K, McClatchey A, Bretscher A, Hewitt SM and Khanna C. Expression of the cytoskeleton linker protein ezrin in human cancers. Clinical & Experimental Metastasis 2007; 24: 69–78. [PubMed: 17370041]
16. Bohling T, Turunen O, Jaaskelainen J, Carpen O, Sainio M, Wahlstrom T, Vaheri A and Haltia M. Ezrin expression in stromal cells of capillary hemangioblastoma. An immunohistochemical survey of brain tumors. American Journal of Pathology 1996; 148: 367–373. [PubMed: 8579099]
17. Ilmonen S, Vaheri A, Asko-Seljavaara S and Carpen O. Ezrin in primary cutaneous melanoma. Modern Pathology 2005; 18: 503–510. [PubMed: 15475929]
18. Krishnan K, Bruce B, Hewitt S, Thomas D, Khanna C and Helman LJ. Ezrin mediates growth and survival in Ewing's sarcoma through the AKT/mTOR, but not the MAPK, signaling pathway. Clinical & Experimental Metastasis 2006; 23: 227–236. [PubMed: 17028919]
19. Weng WH, Ahlen J, Astrom K, Lui WO and Larsson C. Prognostic impact of immunohistochemical expression of ezrin in highly malignant soft tissue sarcomas. Clinical Cancer Research 2005; 11: 6198–6204. [PubMed: 16144921]
20. Seabright M A rapid banding technique for human chromosomes. Lancet 1971; 2: 971–972.
21. Khanna C, Prehn J, Yeung C, Caylor J, Tsokos M and Helman L. An orthotopic model of murine osteosarcoma with clonally related variants differing in pulmonary metastatic potential. Clinical and Experimental Metastasis 2000; 18: 261–271. [PubMed: 11315100]
22. Khanna C, Khan J, Nguyen P, Prehn J, Caylor J, Yeung C, Trepel J, Meltzer P and Helman L. Metastasis-associated differences in gene expression in a murine model of osteosarcoma. Cancer Research 2001; 61: 3750–3759. [PubMed: 11325848]
23. Selden JR, Moorhead PS, Oehlert ML and Patterson DF. The Giemsa banding pattern of the canine karyotype. Cytogenetics and Cell Genetics 1975; 15: 380–387. [PubMed: 1225497]
24. Karroum A, Mirshahi P, Benabbou N, Faussat AM, Soria J, Therwath A, Mirshahi M and Hatmi M. Matrix metalloproteinase-9 is required for tubular network formation and migration of resistant breast cancer cells MCF-7 through PKC and ERK1/2 signalling pathways. Cancer Letters 2010; 295: 242–251. [PubMed: 20359813]

25. Techasen A, Loilome W, Namwat N, Takahashi E, Sugihara E, Puapairoj A, Miwa M, Saya H and Yongvanit P. Myristoylated alanine-rich C kinase substrate phosphorylation promotes cholangiocarcinoma cell migration and metastasis via the protein kinase C-dependent pathway. Cancer Science 101: 658–665. [PubMed: 20047593]

26. Koivunen J, Aaltonen V, Koskela S, Lehenkari P, Laato M and Peltonen J. Protein kinase C alpha/beta inhibitor Go6976 promotes formation of cell junctions and inhibits invasion of urinary bladder carcinoma cells. Cancer Research 2004; 64: 5693–5701. [PubMed: 15313909]

27. Jimeno A, Rudek MA, Purcell T, Laheru DA, Messersmith WA, Dancey J, Carducci MA,Baker SD, Hidalgo M and Donehower RC. Phase I and pharmacokinetic study of UCN-01 in combination with irinotecan in patients with solid tumors. Cancer Chemotherapy and Pharmacology 2008; 61: 423–433. [PubMed: 17429623]

28. Ajani JA, Jiang Y, Faust J, Chang BB, Ho L, Yao JC, Rousey S, Dakhil S, Cherny RC, Craig C and Bleyer A. A multi-center phase II study of sequential paclitaxel and bryostatin-1 (NSC 339555) in patients with untreated, advanced gastric or gastroesophageal junction adenocarcinoma. Investigational New Drugs 2006; 24: 353–357. [PubMed: 16683077]

29. Millward MJ, House C, Bowtell D, Webster L, Olver IN, Gore M, Copeman M, Lynch K, Yap A, Wang Y, Cohen PS and Zalcberg J. The multikinase inhibitor midostaurin (PKC412A) lacks activity in metastatic melanoma: a phase IIA clinical and biologic study. British Journal of Cancer 2006; 95: 829–834. [PubMed: 16969355]

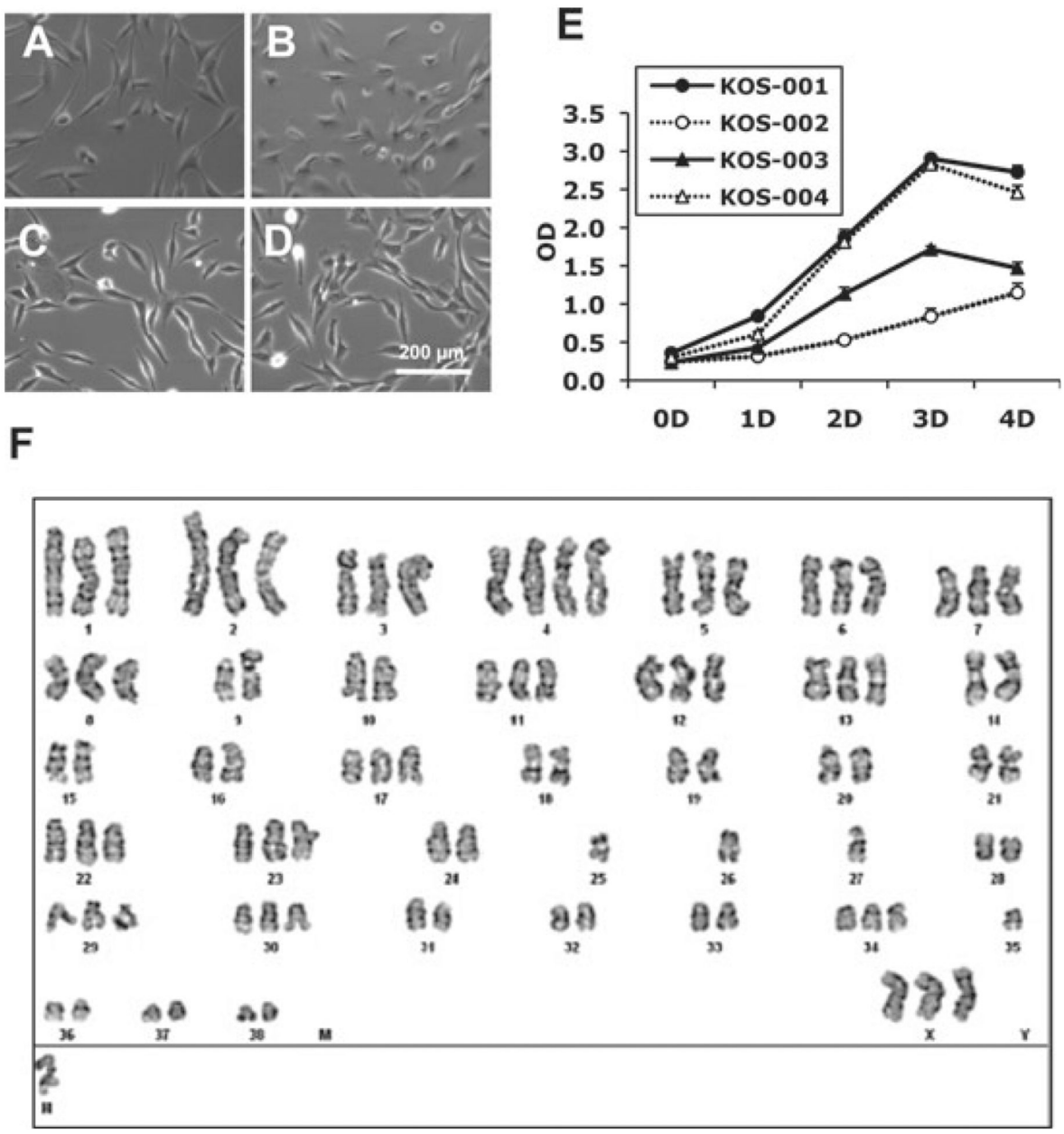

Figure 1.

Canine cell lines have morphological appearance and karyotypic features of osteosarcoma (OS). (A–D) *In vitro* mesenchymal morphologies of canine cell lines. (E) The doubling times of KOS-001, KOS-002, KOS-003 and KOS-004 were 19.8, 24.7, 16.0 and 12.1 h, respectively. (F) Representative G-banding karyotype of canine (KOS-002) OS cells reveals marked aneuploidy. Similar complex and bizarre karyotypes were seen in all other cells. KOS-001, KOS-002, KOS-003 and KOS-004 cell line showed karyotype range 97–105 (mode number was 101), 87–95 (mode number was 95), 81–82 (mode number was 81) and 96–103 (mode number was 103), respectively. Scale bar = 200 μm.

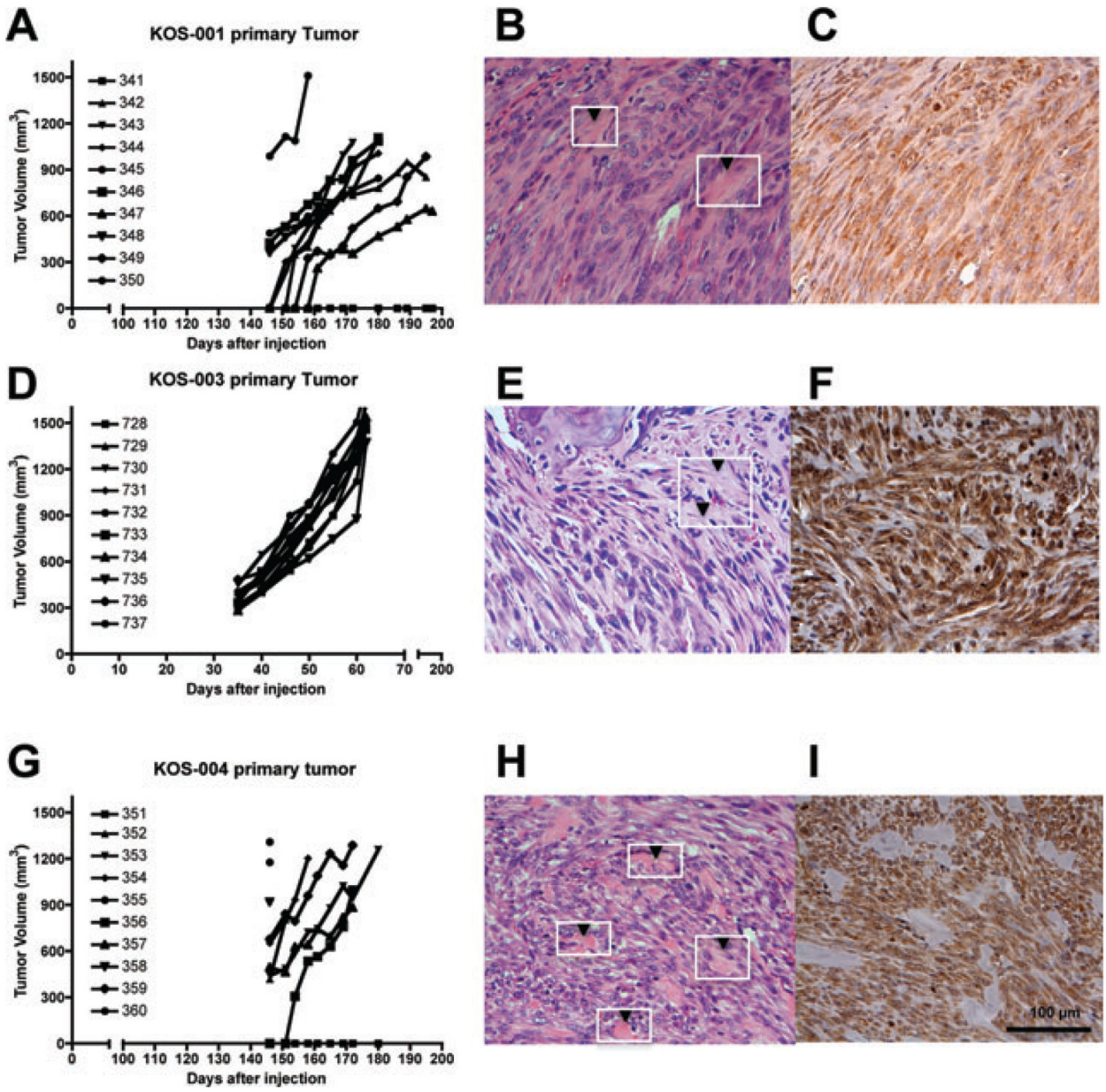

Figure 2.

Canine osteosarcoma (OS) cell lines are tumorigenic in mice and yield tumours with histological descriptors characteristic of OS. (A,D,G) Primary tumour growth patterns of canine OS cells in Beige-SCID mice. Each line represents growth of an individual mouse. H&E staining (B,E,H) of primary tumour resulting from orthotopic injection of KOS-001, KOS-003 and KOS-004 cell lines showed streams of closely packed spindloid tumour cells within a fibrous stroma and small islands of osteoid (see arrow heads) are scattered between the tumour cells. (C,F,I) Primary tumours of KOS-001, KOS-003 and KOS-004 cell lines showed positive ALP staining. Scale bar = 100 µm.

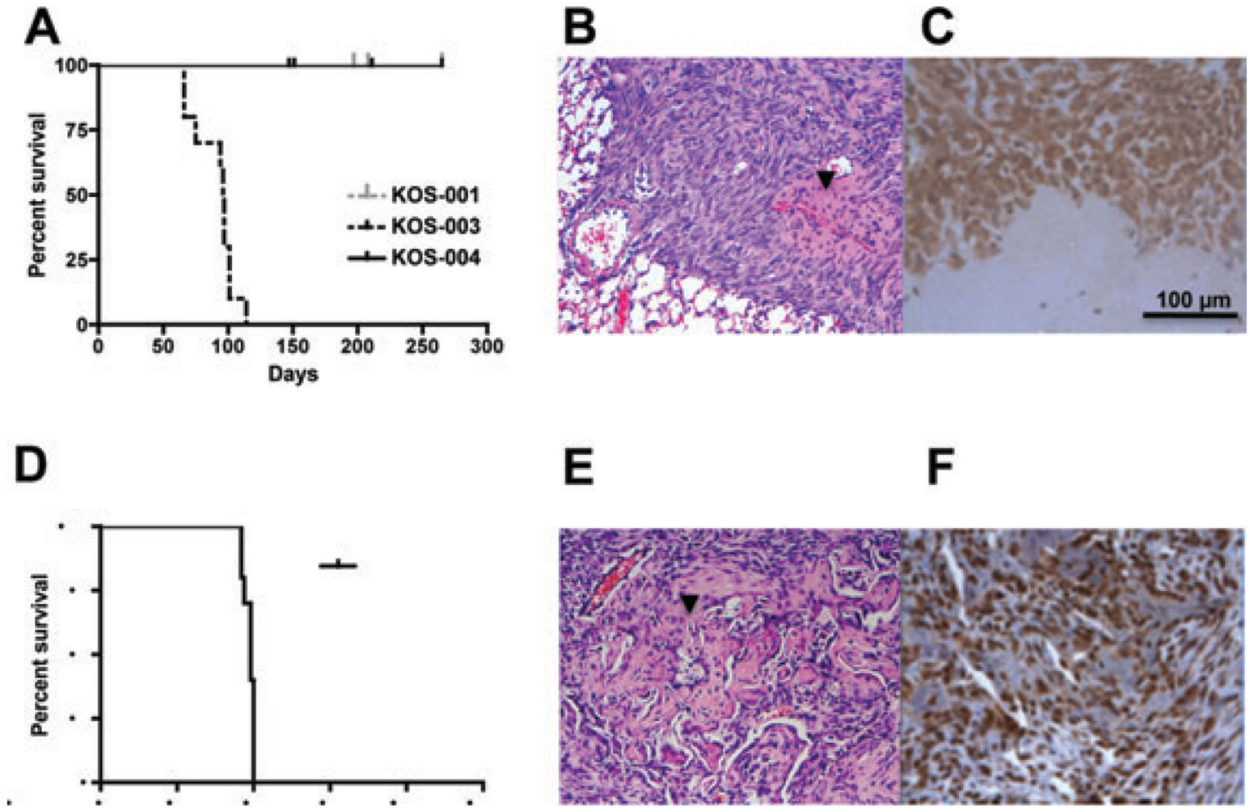

Figure 3.

Assessment of *in vivo* metastatic phenotype of canine osteosarcoma (OS) cell lines. Overall survival of canine OS cells in xenograft metastasis model. (A) Kaplan–Meier survival curves demonstrate progression to spontaneous metastasis in KOS-003 cells following orthotopic delivery of tumour cells to mice. No spontaneous pulmonary metastases were seen in KOS-001 and KOS-004 over 1-year observation period. (B) H&E staining of the resultant metastases were consistent with OS. (C) Spontaneous lung metastasis tumours showed positive ALP staining. (D) The metastatic biology of the KOS-003 was confirmed using experimental metastasis via tail vein injection. (E) H&E staining of experimental metastasis again show osteoid production (arrow head) and (F) ALP staining. Scale bar = 100 μm.

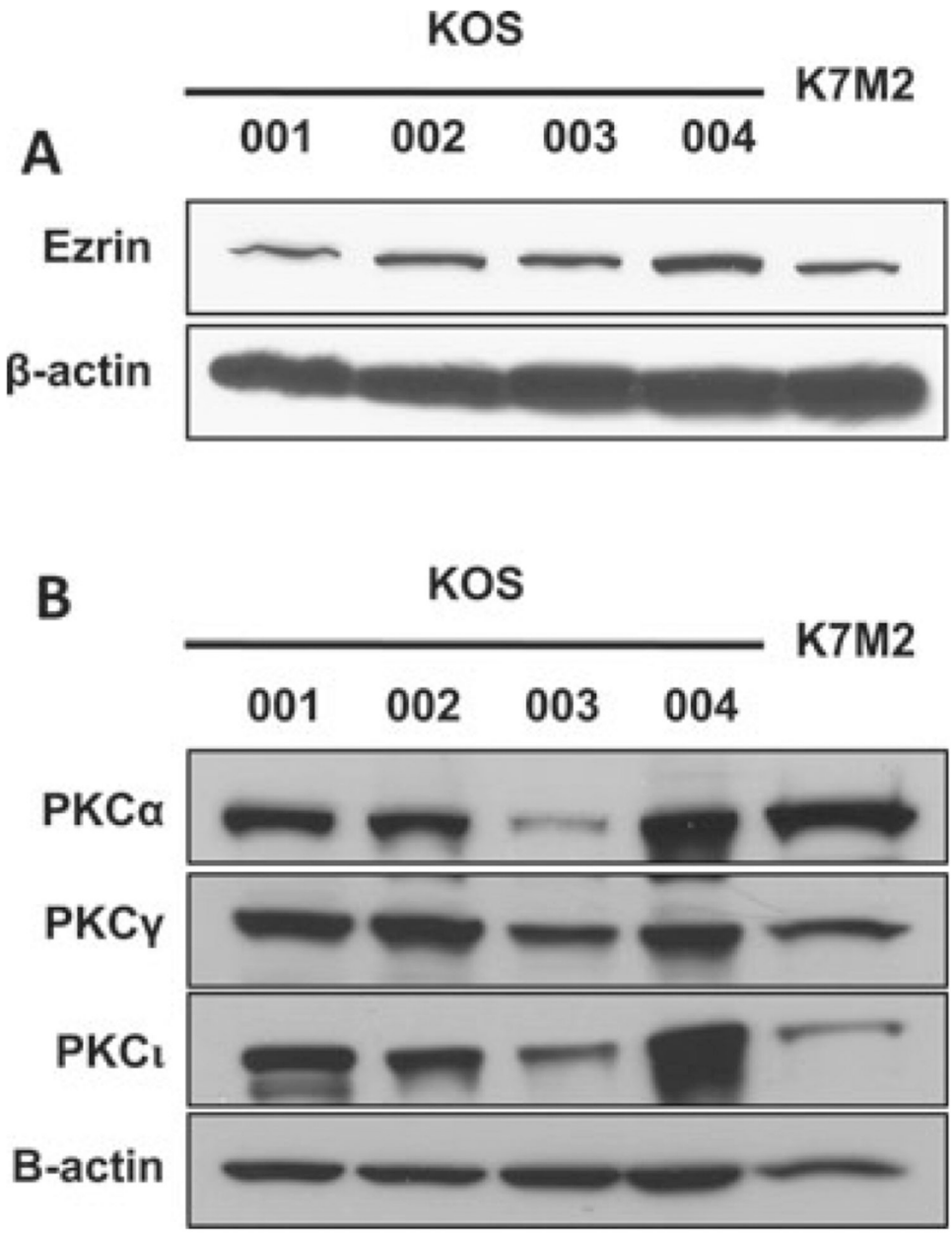

Figure 4.

Ezrin and PKC were expressed in all of canine osteosarcoma (OS) cells. (A) Ezrin was expressed in all of canine OS cells. (B) PKC isoforms α, γ and ι were expressed in all of canine OS cells. K7M2 murine OS cells were used as a positive control.[13]

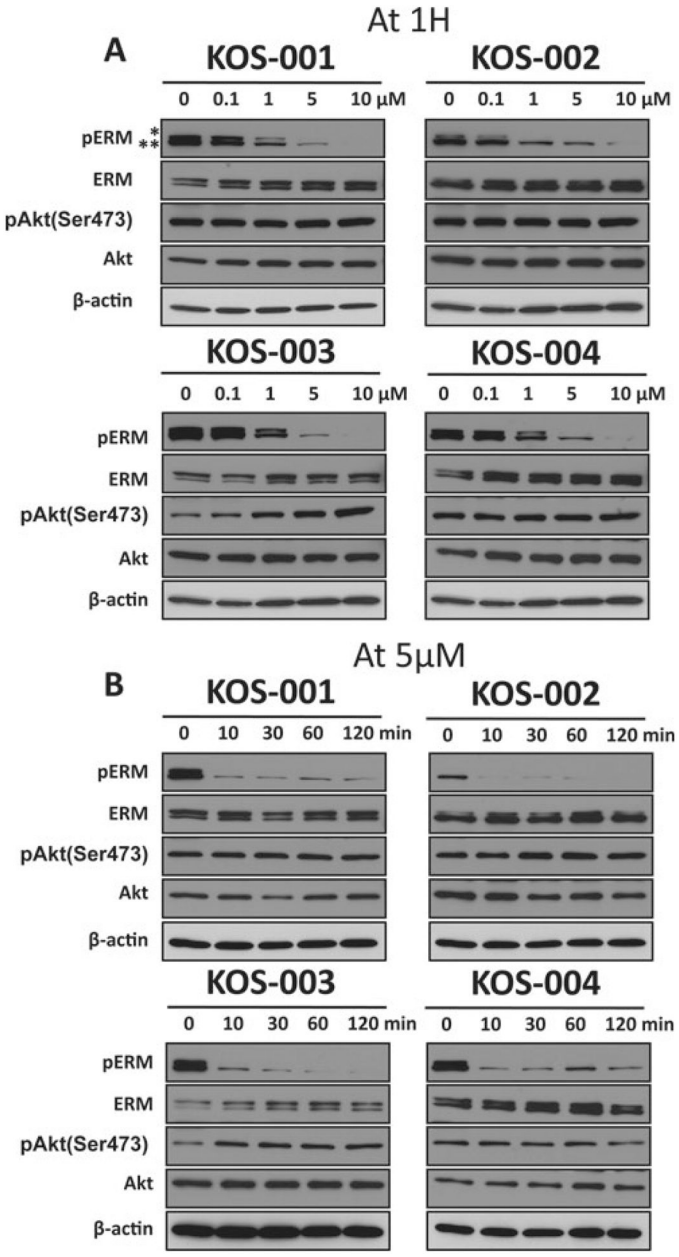

Figure 5.

Ezrin (T567) phosphorylation is dependent on protein kinase C (PKC). (A) Canine osteosarcoma (OS) cells were incubated with various concentrations of PKC inhibitor Ro31–8220. Phospho-ERM expression is shown by western blot analysis (phosphorylated ERM is comprised of a phospho-ezrin/radixin band * and a phospho-moesin band **). (B) Canine OS cells were treated with PKC inhibitors Ro 31–8220 for indicated times. The level of phospho-ERM was analysed by Western blotting. The blots were probed for β-actin as the loading control, and phospho-Akt (Ser473).

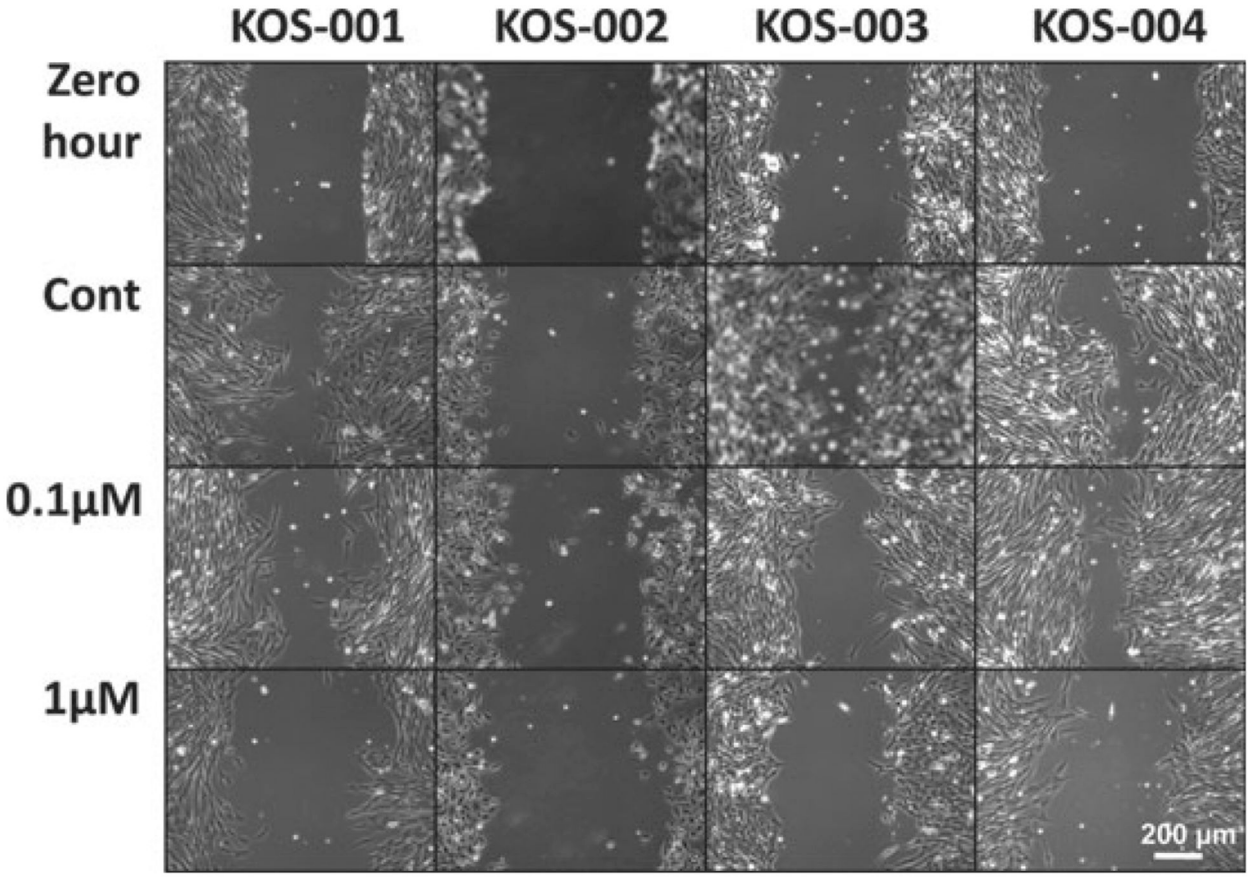

Figure 6.

PKC inhibitors suppress *in vitro* cell migration of canine osteosarcoma cells. Nearly confluent cells were 'wounded' (Scratched) using a P-200 pipette, and images of the denuded area were taken immediately following wounding (0 h) and either 13 or 24 h (KOS-002) after the wound. Migration of KOS-001, KOS-003 and KOS-004 is evident by their migration across the wounded area (Control Migration). Inhibition of this migration is seen following exposure to 0.1 and 1 μM PKC inhibitor, Ro 31–8220. The specific effects of PKC inhibition on cell migration were assured through the selection of drug exposures that did not influence cell viability or proliferation (data not shown) and at times points less than the doubling times of each cell line. The native migration rate of KOS-002 even after 24 h was very low and consistent with its observed low-aggressive phenotype. Scale bar = 200 μm.

Table 1.

Clinical history of canine OS cell lines

Cell line	Chemotherapy	Age	Breed	Tumour location	Lung metastasis	Survival (days)
KOS-001	Carboplatin + OncoLAR	7 years 7 months	Border collie mix	Right distal femur	Metastasis	243
KOS-002	Carboplatin	7 years	Irish setter	Left distal radius	Metastasis	152
KOS-003	Carboplatin + OncoLAR	7.5 years	Lab mix	Right distal radius	Metastasis	232
KOS-004	Carboplatin	8 years	Mixed breed	Left distal radius	Metastasis	268

Table 2.

Summary of *in vivo* tumour growth and lung metastasis of canine OS cell lines

Cell line	% Tumour take[a]	Tumour latency[b] (days)	Tumour growth (days)[c]	Spontaneous metastasis (%)
KOS-001	90% (9/10)	151 ± 6	183 ± 14	0% (0/9)
KOS-002	0% (0/10)	NA	NA	NA
KOS-003	100% (10/10)	35 ± 0	62 ± 0	100% (10/10)
KOS-004	90% (9/10)	147 ± 3	162 ± 14	0% (0/9)

[a]Percent of mice that develop primary tumours following paraoseous injection of 2 million cells to Beige-SCID mice.

[b]Median time (days) to tumour detection.

[c]Median time (days) for tumour to grow to 1.5 cm in diameter.